Modelling and Design of a spherical parallel manipulator for friction-stir welding of Aluminium alloy plates

U.Sudhakar, Dr.J.Srinivas

Abstract

This paper presents the kinematic modelling of a robust parallel manipulator for friction-stir welding application of aluminium alloys and gives some stiffness considerations of the linkage. The mechanism can be used as an alternative platform for conventional friction-stir welding machines. Based on the work carried out on a vertical milling machine for welding the Al-alloy samples, it was found that minimum three degrees of freedom are necessary at the tool-tip for providing necessary huge axial force. A tool-head having three-degree of freedom in space is modelled based on a 3-UPS –PU redundant spherical parallel mechanism. It provides two rotations and one translation at the moving platform. Initially, the kinematics and Jacobian analysis of the mechanism is described. The forward and inverse kinematics are explained. The dexterity and stiffness indices of the mechanism are predicted and mechanism design strategy is presented. Tool-head capabilities in terms of orientation work-volume are also illustrated.

Keywords: Friction-stir welding, Spherical manipulator mechanism, Kinematics and stiffness indices.

1 Introduction

Due to increasing demand of welding of lighter weight material, several cost-effective joining techniques have been evolved during the last one decade. Solid-state joining techniques like friction welding, friction cladding and friction-stir welding would replace the conventional fusion welding processes for Aluminium alloys. Friction-stir welding (FSW) was invented in 1991 by welding institute in UK. Here, a rotating tool with a specially designed shoulder and probe is pressed over the work piece surface at the junction and traversed along the interface with a weld-speed. Due to friction between the rotating tool and work piece, the plastic deformation occurs and temperature rises. The generated heat softens the work piece and yield strength of base material reduces. As tool is moved from one location to other, the momentary softening at each instant of time will form the weld. Friction-stir welding can be used to join dissimilar alloys and metals. It results in excellent weld strength, ductility and toughness.

During FSW, the weld quality is affected by various parameters. It results in changes of different mechanical properties of work-material. Literature reports several applications of FSW in marine and defence industries [1-5]. Main advantage of the process is that it is free from oxide formation and welding cracks. Also, there are low residual stresses due to relatively small input energy. All the FSW works focussed on the

U.Sudhakar
Department of Mechanical Engineering, GMR IT-Rajam, E-mail:mr.u.sudhakar@gmail.com

Dr.J.Srinivas (Corresponding author)
Department of Mechanical Engineering, NIT Rourkela 769008, E-mail:srin07@yahoo.co.in.

following areas: (i) studies on effects of operating parameters on mechanical, thermal and fluid properties of weld (ii) studies relating to similar/dissimilar workpiece materials (iii) studies on influences of type of tool probe (like square headed or triangular headed etc) on the mechanical characteristics of resulting weld etc. Few studies are also found on (a) immersed friction-stir welding [6] (b) counter-rotating or fixed shoulder friction-stir welding [7] (c) an alternative type of the machine/mechanism to guide the tool and fixture used for grip the work pieces during welding.

Present paper focuses on the approach of using a suitable manipulator to guide the rotating tool in the work piece plane. Such an approach is more convenient for light weight materials including polymers and low thickness aluminium alloys. An observer based adaptive control scheme for axial force control in friction-stir welding was proposed by Davis et al. [8], where the force-estimation using instantaneous power measurements has been illustrated. Jain et al.[9] proposed an optimal work placement analysis for friction stir welding using 6-axis serial robot configurations. More recently, Backer [10] elaborated the path deviations occurring in friction-stir welding process with an online visual tracking system for a serial robot based tool head. Memdes et al.[11] presented a friction stir welding platform design for polymer materials and illustrated its operation using a six degree of freedom serial manipulator with hybrid force and motion control. Now-a-days, parallel robots have become attractive alternatives in applications like machine tools, motion simulators, and micro-scale positioning system as well as in medical devices. Main benefits of using parallel manipulators are their high payload ability, good stiffness and accuracy. Further, compared to industrial serial joint robots, here the end-effector errors are relatively small due to the parallel configuration. Recently many works, illustrated the design of friction-stir welding platforms based on parallel kinematic machines. Shi et al. [12] proposed 3-PRS parallel mechanism for friction-stir welding operation. Li et al.[13] implemented a 5-axis hybrid manipulator to maintain huge downward force. It has 2-SPR-RPS parallel manipulator on a gantry structure.

In this perspective, initially, 5 mm thick aluminium alloy plates are considered for welding using conventional column and knee type milling machine. A constant axial downward force is applied and the effects of speed (tool rotation) and feed (weld speed) are studied on mechanical properties including impact strength and hardness of weld. After knowing the required degrees of freedom and minimum axial force, a parallel manipulator-based linkage is proposed to achieve the requirements. Kinematics and stiffness issues of a 3-degree of freedom spherical parallel manipulator mechanism are described mathematically. The results help in analysing the practical functioning of the mechanism towards friction-stir welding applications.

2 Description of platform and kinematics

Application of multi-axis industrial robots in FSW has became quite common. It is proposed to use a redundant 3-UPS- PU parallel mechanism having a moving tripoid supported by fixed base platform through three active legs and one passive leg at the center (see Fig.1). Each of the three active legs of the linkage consists of a passive universal (U), actuated prismatic (P) and passive spherical (S) joints from fixed base to moving platform direction. This standard 3-UPS linkage posseses six degrees of freedom [14] as per Grubler-Kutzbach criterion. The redundant passive leg is made-

up of a prismatic (P) and universal (U) joint (at moving platform) and has X and Y translations and a rotation about Z-axis. Thus, the moving platform has in total three-degrees of freedom (2 rotations about X, Y directions and one translation about Z direction).

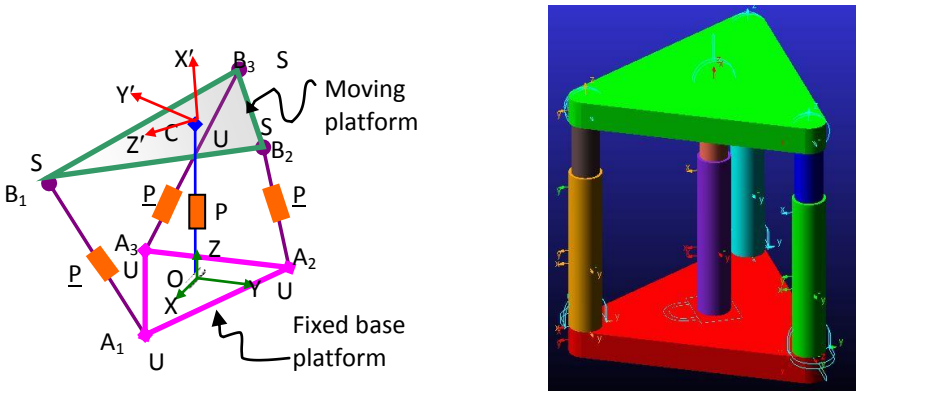

(a) Line diagram (b) solid model in ADAMS

Figure 1. Redundant 3-RPS Parallel mechanism

Joint angles are obtained at every position on the trajectory using inverse kinematics. This is based on geometric vector approach. Let a fixed coordinate frame X-Y-Z and moving coordinate frame X′-Y′-Z′ are respectively attached to the base and mobile platforms. If the position vectors of points B_1, B_2 and B_3 (with respect to moving frame) and the coordinates of base platform A_1, A_2 and A_3 (referring to fixed frame X-Y-Z) are known at any pose, it is possible to obtain the inverse kinematics as follows:

The vector length of each prismatic actuator (P) is given by the vector [15]:

$$\rho_i = OB_i - OA_i = [R]CB_i + OC - OA_i \text{ , i=1,2,3} \quad (1)$$

Here, [*R*] is a rotation matrix defining orientation of the coordinate frame x′y′z′ with respect to xyz frame and is given in terms of Euler angles θ_x, θ_y and θ_z as:

$$[R] = \begin{bmatrix} c_z c_y & -c_x s_z + c_z s_y s_x & s_x s_z + c_z s_y c_x \\ s_z c_y & c_z c_x + s_z s_y s_x & -c_z s_x + s_z s_y c_x \\ -s_y & c_y s_x & c_y c_x \end{bmatrix} \quad (2)$$

where *c* and *s* are cosine and sine functions. The suffixes x, y and z respectively denote the cosine and sine of θ_x, θ_y and θ_z (for eg., c_x=cos θ_x etc). Due to extra redundant link (leg), the moving platform has θ_z=0 and the position vector *OC* =$[0\ 0\ z]^T$. Further, the triangles $B_1B_2B_3$ and $A_1A_2A_3$ are considered as equilateral triangles inscribed in two circles of radii *b* and *a* respectively. By expanding the expressions in Eq.(1), we get:

$$\rho_i = \begin{Bmatrix} (B_{yi} s_x s_y + B_{zi} c_x s_y - A_{xi}) \\ (B_{yi} c_x - B_{zi} s_x - A_{yi}) \\ (s_x c_y B_{yi} + c_x c_y B_{zi} + z) \end{Bmatrix} \quad \text{i=1,2,3} \quad (3)$$

Here, (A_{x1},A_{y1},0), (A_{x2},A_{y2},*0*), (A_{x3},A_{y3},*0*) are coordinates of A_1, A_2 and A_3 with respect to centre O of the coordinate frame xyz, while (0,B_{y1},B_{z1}), (0,B_{y2},B_{z2}) and (0,B_{y3},B_{z3}) are the coordinates of B_1, B_2 and B_3 with respect to centre C of moving frame x′y′z′ respectively. The equation (3) results in the inverse kinematics as

$$\rho_i^2(\theta_x,\theta_y,z) = D_{1i}^2 + D_{2i}^2 + D_{3i}^2,\ i=1,2,3 \tag{4}$$

The following Jacobian matrix can be obtained by taking time-derivative on both sides:

$$\rho_i\dot{\rho}_i = E_{1i}\dot{\theta}_x + E_{2i}\dot{\theta}_y + E_{3i}\dot{z} \tag{5}$$

where

$$\begin{aligned} E_{1i} = &[(s_x s_y B_{yi} + c_x s_y B_{zi} - A_{xi})(c_x s_y B_{yi} - s_x s_y B_{zi}) \\ &+(c_x B_{yi} - s_x B_{zi} - A_{yi})(s_x B_{yi} + c_x B_{zi}) \\ &+(z + s_x c_y B_{yi} + c_x c_y B_{zi})(c_x c_y B_{yi} - s_x c_y B_{zi})] \end{aligned} \tag{6}$$

$$\begin{aligned} E_{2i} = &[(s_x s_y B_{yi} + c_x s_y B_{zi} - A_{xi})(s_x c_y B_{yi} + c_x s_y B_{zi}) \\ &-(z + s_x c_y B_{yi} + c_x c_y B_{zi})(s_x s_y B_{yi} + c_x s_y B_{zi})] \end{aligned} \tag{7}$$

$$E_{3i} = (s_x c_y B_{yi} + c_x c_y B_{zi} + z) \tag{8}$$

Equation (5) can be written in matrix-form as:

$$\begin{bmatrix} \rho_1 & 0 & 0 \\ 0 & \rho_2 & 0 \\ 0 & 0 & \rho_3 \end{bmatrix} \begin{Bmatrix} \dot{\rho}_1 \\ \dot{\rho}_2 \\ \dot{\rho}_3 \end{Bmatrix} = \begin{bmatrix} E_{11} & E_{21} & E_{31} \\ E_{21} & E_{22} & E_{23} \\ E_{31} & E_{32} & E_{33} \end{bmatrix} \begin{Bmatrix} \dot{\theta}_x \\ \dot{\theta}_y \\ \dot{z} \end{Bmatrix} \tag{10}$$

This is something like: $[J_q]\{\dot{q}\} = [J_X]\{\dot{X}\}$.Obviously, the first type of singularities occur when determinant of [J_q]=0, where the platform loses one or more degrees of freedom. The second type happens when determinant of [JX]=0, which states that the platform gains one or more degrees of freedom (platform moves even no actuation is applied leading to zero stiffness). The resultant nonlinear kinematic equation describing input-output relationship may be finally written as:

F (ρ, θ_x, θ_y, z)=0.

A set of space configurations reachable by the end-effector is defined by the limits imposed on the Prismatic joints. The well conditioned workspace is then determined. Jacobian matrix [J] =$[J_q]^{-1}[J_X]$ at a particular pose/posture requires a sort of homogenization as its elements are expressed in different units. Topology of the structure and pose of mobile platform within the workspace defines the stiffness. The stiffness matrix combines the forces and moments applied to end-effector and is defined as: [K]=k[J][J]^T, where k is actuators' stiffness. The maximum and minimum eigenvalues of this matrix correspond to the maximum and minimum stiffness values. To have best possible rigidity, we select the minimum eigenvalue of the matrix. That is minimum payload capability of the platform should be made larger. In order assess the dexterity and stiffness over the entire workspace, we taken the global indices defined over the volume interval

3 Results and Discussion

The position and stiffness analysis of manipulator are illustrated with a case.

The parameters considered for analysis are shown in Table-1.

Table 1. Platform and actuator parameters

Parameter	Value
Radius of base paltform (a)	0.18 m
Radius of moving platform (b)	0.12 m
Height of platform (z)	0.5 to 0.7 m
Joint stiffness (*k*)	1000 N/m
Prismatic actuator stroke range	[0.2, 0.6]

The work volume, kinematic indices and the stiffness index are obtained by providing the radii of platforms as well as the maximum and minimum values of strokes of prismatic actuators as input. Fig.2 shows the work volume in three-dimensional θ_x-θ_y-z space.

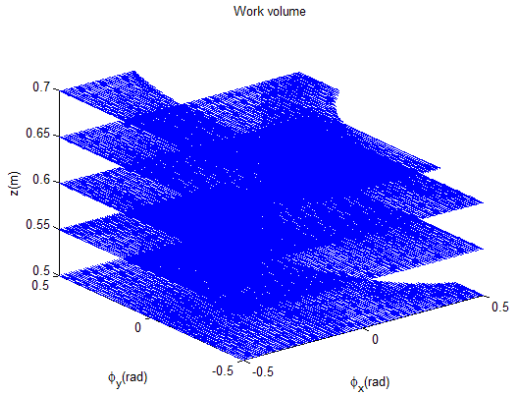

Fig.2 Work volume

Fig.3 depicts the orientation workspace at different values of z as a polar plot.

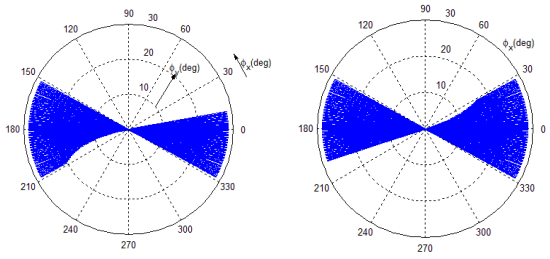

Fig.3 Orientation workspace at (i) z=0.5 (ii) z=0.65m

It is seen that at certain lower/higher heights, there exists a limited usable workspace. Fig.4 shows the dexterity in terms of conditioning index at two different z locations

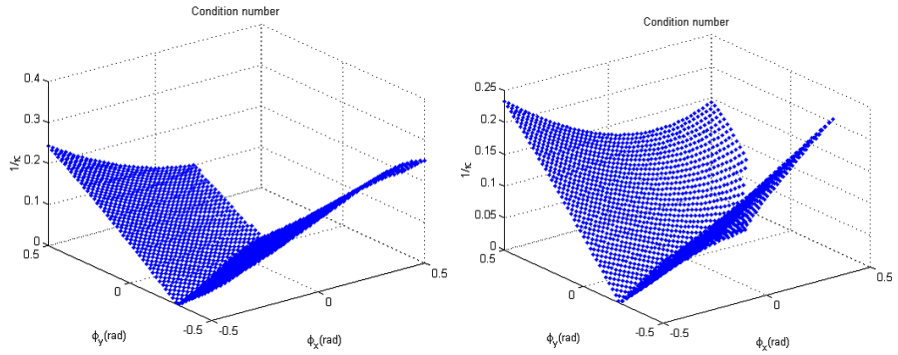

(i) z=0.5 m (ii) z=0.65 m

Fig. 4 Conditioning index at two different z locations

Further, the payload or stiffness index in terms of lowest eigenvalue of stiffness matrix at the posture is illustrated in Fig.5.

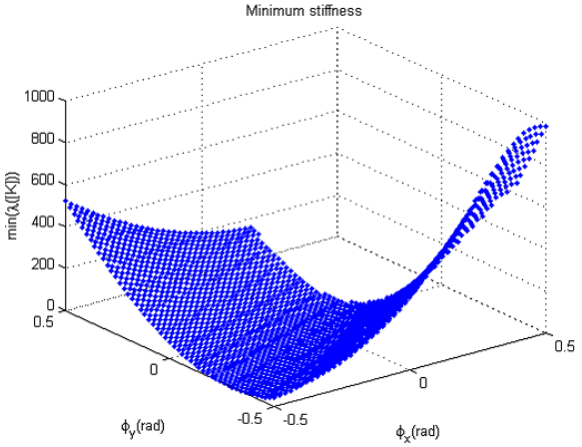

(i) z=0.5 m

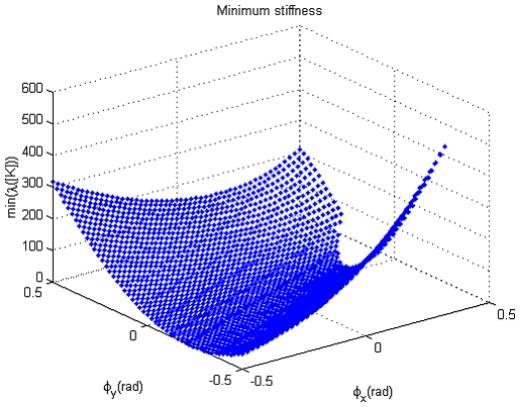

(ii) z=0.65 m

Fig.5 Variation of lowest eigenvalue of stiffness matrix

Interestingly, at certain poses, there exists singularities and manipulator losses the stiffness as seen from these figures at both values of z. In such instances, the passive redundant leg helps to overcome by providing additional motion to platform. Based on these indices, it is possible to design the optimum platform dimensions, such that both these global indices should reach their maxima, under certain variable constraints. Friction welding tool can be placed confidently on the optimized platform center, to withstand the static wrench forces during the welding operation. Both the motion and force (hybrid) control task is required while tracking the required trajectories.

4 Conclusions

An experimental platform for conducting friction-stir welding has been described in this work. By providing careful fixtures and controlling operating variables like work feed and tool speed, one can use conveniently the milling machine itself for the welding operation. However, milling machine dynamics plays an important role in precision welding during thin component-joining. Therefore, present work has explored on the possibilities of utilizing redundant spatial manipulators for friction-stir welding. The kinematics and stiffness analysis of a 3-UPS-PU parallel mechanism was briefly described and variation of stiffness index was illustrated within the work-volume. Operations of prismatic actuators require a model based control and the work is under progress.

References

[1] H.K.Mohanty M.M.Mahapatra, P.Kumar, P. Biswas and N.R.Mandal, “Predicting effects of tool geometries on friction stir Aluminum welds using aritificial neural networks and fuzzy logic techniques”. Int. J. Manuf..Research, vol.8, pp.296-312, 2013.

[2] K.Kuykendall, T.Nelson, C.Sorensen, “On the selection of constitutive laws used in modeling friction stir welding”, Int.J.Mach.Tools and Manuf. vol.74, pp.74-85, 2013.

[3] P.T.C.Prasad, P.Hema, K. Ravindranath, “Optimization of process parameters for friction stir welding of Al-alloy AA6061 using square pin profile”, Int.J.Mech.Engg. and Robotic Research, vol.3, pp.455-465, 2014.

[4] B.T.Gibson, D.H.Lammlein, T.J.Prater, W.R.Longhurst, C.D.Cox, M.C.Ballun, K.J.Dharmaraj, G.A.Cook, A.M.Strauss, “Friction-stir welding: Process, automation and control”. J. Manf. Processes, vol.16, pp.56-73, 2014.

[5] S.T.Selvamani, K.Palanikumar, K.Umanath, D.Jayaperumal, “Analysis of friction-stir welding parameters on the mechanical metallurgical and chemical properties of AISI 1035 steel joints”, Materials and Design, vol.65, pp.652-661, 2015.

[6] M.Hosseini, H.D.Manesh, “Immersed friction stir welding of ultrafine grained accumulative roll-bonded Al-alloy”, Materials and Design, vol.31, pp.4786-4791, 2010.

[7] D.Li, X.Yang, L.Cui, F.He, X.Zhang, “Investigation of stationary shoulder friction stir welding of aluminium alloy 7075-T651”, J.Mat.Proc.Tech. vol.222, pp.391-398, 2015.

[8] T.A.Davis, Y.C.Shin, B.Yao, "Observer-based adaptive robust control of friction-stir welding axial force", Proc. IEEE/ASME Int. Conf. Adv. Int. Mechatronics, Montreal, Jul 6-9, 2010, pp.1162-1167.

[9] A.Jain, J.Qin, G.Abba, "Optimal work placement for robotic friction stir welding task", Proc. Third IFToMM Int. Sym. Robotics and Mechatronics, Singapore, 2-4 Oct 2013.

[10] J.D.Backer, *Feedback control of robotic friction-stir welding*, Ph.D.Thesis, Univesity West, 2014.

[11] N.Mendes, P.Neto, M.A.Simao, A.Lourciro, "A novel friction stir welding robotic platform: welding polymeric materials", Int. J. Adv. Manuf. Technol. DOI 10.1007/s00170-014-6024-z..

[12] J.Shi, Y.Wang, G.Zhang, H.Ding, "Optimal design of 3-DOF PKM module for friction stir welding", Int. J.Adv.Manuf.Technol. vol.66, pp.1879-1889, 2013.

[13] Q.Li, W.Wu, J.Xiang, H.Li, C.Wu, "A hybrid robot for friction-stir welding", J.Mechanical Engg., Sciences, Part-C, Proc.IMech E., doi: 10.1177/0954406214562848

[14] Y.Lu, P.Wang, Z.Hou B.Hu, C.Sui J.Han, "Kinetostatic analysis of a novel 6-DOF 3UPS parallel manipulator with multi-fingers", Mechanisms and Mach. Theory, Vol.78, pp.36-50, 2013.

[15] G. Alici and B. Shirinzadeh, "Loci of singular configurations of a 3-DOF spherical parallel manipulator", Robotics and Autonomous Systems. vol.48, pp.77-91, 2004.